Energy Conversion and Management 85 (2014) 361–372

Contents lists available at ScienceDirect

Energy Conversion and Management

journal homepage: www.elsevier.com/locate/enconman

Multi-objective optimization of two alkali catalyzed processes for biodiesel from waste cooking oil

Dipesh S. Patle [a], Shivom Sharma [b], Z. Ahmad [a,*], G.P. Rangaiah [b]

[a] School of Chemical Engineering, Engineering Campus, Universiti Sains Malaysia, Nibong Tebal, Penang 14300, Malaysia
[b] Department of Chemical & Biomolecular Engineering, National University of Singapore, Engineering Drive 4, Singapore 117576, Singapore

ARTICLE INFO

Article history:
Received 19 March 2014
Accepted 10 May 2014
Available online 19 June 2014

Keywords:
Biodiesel
Waste cooking oil
Multi-objective optimization
Elitist non-dominated sorting genetic algorithm
MS Excel

ABSTRACT

In view of the finite availability and environmental concerns of fossil fuels, biodiesel is one of the promising fuel alternatives. This study considers waste cooking palm oil with 6% free fatty acids (FFA) as feed-stock, which facilitates its better utilization and promotes sustainability. Two biodiesel production processes (both involving esterification catalyzed by sulfuric acid and trans-esterification catalyzed by sodium hydroxide) are compared for economic and environmental objectives. Firstly, these processes are simulated, considering detailed constituents of palm oil and also detailed kinetics for both esterification and trans-esterification, in Aspen Plus simulator. Subsequently, both the processes are optimized considering profit, heat duty and organic waste as objectives, and using an Excel-based multi-objective optimization (EMOO) program for the elitist non-dominated sorting genetic algorithm-II (NSGA-II). The results show that the profit improves with the increase in heat duty, and that the profit increase is accompanied by larger amount of organic waste. Process 1 having three trans-esterification reactors produces significantly lower organic waste (by 32%), requires lower heat duty (by 39%) and slightly more profitable (by 1.6%) compared to Process 2 having a single trans-esterification reactor and also a different separation sequence. Overall, the obtained quantitative trade-offs between objectives enable better decision making about the process design for biodiesel production from waste cooking oil.

1. Introduction

All over the world, there is an increasing interest on the production of biodiesel due to its eco-friendliness and renewability. Biodiesel has a higher flash point that makes it more suitable for transportation and handling. Also, it has a more favorable combustion emission profile than petroleum diesel, such as lower emissions of carbon monoxide, particulate matter and unburned hydrocarbons [1].

Biodiesel production from WCO is attractive for both economic and environmental reasons since WCO is cheaper than vegetable oils and its direct disposal to the environment has adverse impacts [2]. Although trans-esterification is more efficient and faster with an alkali catalyst compared to an acid catalyst, high amount of FFA in WCO produces soap in the presence of an alkali catalyst [3]. Hence, alkali-catalyzed process cannot directly be used to produce biodiesel from WCO. To increase the formation of FAMEs (i.e., biodiesel) by trans-esterification, Freedman et al. [4] recommended using refined vegetable oils with an FFA content lower than 0.5% (w/w), methanol to oil molar ratio of 6:1, and reaction temperature of about 333 K. Also, water content of vegetable oils should be kept below 0.06% (w/w) [5]. WCO typically contain 2%–7% of FFAs [6]. In these cases, an acid catalyst such as sulfuric acid can be used to esterify FFAs to FAMEs, thus reducing FFA content of feed. Pre-treated oil can then be trans-esterified with an alkali-catalyst to obtain FAMEs. Accordingly, Canakci and Van Gerpen [7] proposed a two-step process, esterification followed by trans-esterification, to produce biodiesel.

Zhang et al. [8] proposed four biodiesel production processes, namely, alkali-catalyzed process using pure vegetable oil, alkali-catalyzed process using WCO, acid-catalyzed process using WCO, and acid-catalyzed process using hexane extraction. Later, Zhang et al. [9] performed economic analysis and found that the acid-catalyzed process using WCO is more economical compared to others studied. West et al. [10] conducted economic analysis of four biodiesel production processes, using WCO as feed-stock; these include acid-catalyzed, alkali-catalyzed, heterogeneous acid-catalyzed and supercritical processes. They concluded that heterogeneous acid-catalyzed process is more economical than others, but it is still in the development phase. Talebian-Kiakalaieh et al.

* Corresponding author. Tel.: +604 599 6462; fax: +604 594 1013.
E-mail address: chzahmad@usm.my (Z. Ahmad).

http://dx.doi.org/10.1016/j.enconman.2014.05.034
0196-8904/

[11] reported that utilization of waste cooking oil can reduce biodiesel production cost by 60–90%.

With increasing economic competition and scarcity of resources, there is greater need for optimization of chemical processes. Four alkali-catalyzed biodiesel processes having different separation sequences were optimized by Myint and El-Halwagi [12]. They found that biodiesel and glycerol separation should be performed first, followed by methanol recovery and water washing. Nicola et al. [13] optimized two slightly different alkali-catalyzed biodiesel processes for energy consumption and product quality, using genetic algorithm. Martin and Grossmann [14] carried out simultaneous optimization and heat integration of different technologies for the trans-esterification of oil. They formulated the problem as a mixed integer nonlinear programming (MINLP) problem, where the models for each of the reactors are based on response surface methodology (RSM) to capture the effects of process variables on the yield. Huerga et al. [15] presented an integrated process to obtain biofuels from *Jatropha curcas* crop. They performed several experiments to optimize the process diminishing the consumption of methanol and catalysts.

Sharma and Rangaiah [16] optimized biodiesel production from WCO for multiple objectives, using multi-objective differential evolution. They considered both esterification and trans-esterification steps, and three continuous stirred tank reactors (CSTR) in series for trans-esterification, which has obvious advantages. Fauzi and Amin [17] optimized oleic acid esterification catalyzed by ionic liquid. They used RSM based on central composite design for single-objective optimization, while artificial neural network with genetic algorithm was employed for simultaneous optimization of responses to the reaction conditions. Rahimi et al. [18] studied the optimization of biodiesel production from soybean oil in a microreactor. They used Box–Behnken method and RSM for the optimization of molar ratio of methanol to oil, catalyst concentration and temperature. Ong et al. [19] optimized biodiesel production from *Calophyllum inophyllum* oil containing high free fatty acid.

In the literature on multi-objective optimization (MOO) of biodiesel production from WCO, detailed esterification and trans-esterification kinetics for a mixture of glycerides are not considered. Most of the previous studies [1,8–10,12,16,20,21] use a single triglyceride/FFA and FAME to represent the vegetable oil and biodiesel, respectively. Further, fixed conversions of FFA and triglyceride into FAME were often assumed [1,8,9,20]. It is better to avoid these in order to obtain realistic results, particularly for comparing plant performance for various feed-stocks. In this direction, Garcia et al. [22] considered three triglycerides to represent vegetable oil, but mono- and di-glyceride intermediates were neglected in the reaction. Unlike previous studies, the present study simulates the two process alternatives for biodiesel production from WCO considering detailed constituents of WCO and detailed kinetics (esterification and trans-esterification are represented by 10 and 96 kinetic reactions, respectively). The two alternate designs are optimized and compared for both economic and environmental interests, using maximum profit, minimum heat duty and minimum organic waste as objectives. Both the process alternatives use alkali-catalyzed trans-esterification, which is more efficient and also used in industrial practice [23,24]. Process 1 is based on the process flow sheet in Sharma and Rangaiah [16], where methanol removal is followed by water washing. Process 2 is based on the process flow sheet presented by Morais et al. [1], where water washing is followed by separation of products. Note that Morais et al. [1] did not carry out optimization, which is necessary to obtain the maximum benefits. In order to make the two process alternatives comparable, some modifications are made to them, which are presented in the next section. This study considers the sequential approach, where a complete process is simulated in Aspen Plus and optimized using Excel-based elitist non-dominated sorting genetic algorithm (NSGA-II). Effect of using detailed oil components versus a lumped component is also investigated. Additionally, the quality of biodiesel is evaluated and compared against EN14214. Next section describes the process development.

2. Process development

For the present study, biodiesel plant capacity is assumed to be 120 kt/annum based on the potential WCO availability. The feed is considered to be waste cooking palm oil as palm oil is extensively used in Malaysia for cooking. However, the processes presented below can process WCO as well as crude palm oil (CPO) as they have similar FFA content. Therefore, actual feed can be either WCO or CPO, depending on their availability and costs. The two alternatives for the complete biodiesel process, studied in this work are discussed below.

2.1. Process 1

Fig. 1 shows a process schematic for biodiesel production from WCO, where products separation is followed by water washing [16]. WCO with a flow rate of 15,000 kg/h (stream 'OIL' in Fig. 1) is processed in the esterification reactor (RFFA), where FFAs react with methanol in the presence of acid catalyst to yield FAMEs. The OIL stream is pre-heated in a heat exchanger with the esterification reactor products (stream 'RFFA1'). The esterification is performed at 60 °C, 4 bar pressure, methanol (stream 'MEOH') to FFAs molar ratio of 10:1 and with 10% (w/w) of sulfuric acid relative to FFAs [26]. The esterification products (stream 'RFFA1'), after cooling via pre-heating of WCO, are mixed with glycerol and then sent to the phase separator 'W-1', where sulfuric acid and water are separated from the reaction mixture. Glycerol forms two phases with reaction mixture, and acid catalyst is removed in heavy phase. Stream 'W-1-2' containing mainly glycerol, methanol, water and acid catalyst, from the phase separator 'W-1' goes to a distillation column (FRAC-1) where most of the unreacted methanol is recovered and recycled (stream 'FRAC-1-1'). FRAC-1 column has 8 theoretical stages and operates at reflux ratio of 1. The recycled methanol is then fed back to the esterification reactor (RFFA). Glycerol and sulfuric acid leave the FRAC-1 column in the bottom stream (FRAC-1-2), which is then fed to a neutralization reactor (R-CAO), where sulfuric acid reacts with calcium oxide to produce calcium sulphate (stream 'CAO'). The calcium sulphate produced in the reactor is then removed in a gravity separator (S-1). The glycerol stream (S-1-1) leaving the separator S-1 is further purified in a flash evaporator (F-1), where the remaining methanol and water are removed from the top stream (ME-WAT-1) and treated as a waste stream due to small methanol flow rate of 8.53 kg/h. Finally, glycerol is recycled back and mixed with fresh glycerol, which forms two liquid phases in phase separator W-1. The light phase from separator W-1 includes oil, biodiesel, methanol and water while the heavy phase contains glycerol, catalyst, methanol and water. The pretreated WCO feed stream (W-1-1) is fed to a distillation column (FRAC-2 with 10 theoretical stages and operating at reflux ratio of 1), where most of the unreacted methanol (stream 'FRAC-2-1') is recovered in the distillate stream and recycled to the esterification reactor 'RFFA'.

The bottom stream 'FRAC-2-2' containing FAMEs and unreacted oil is processed in the trans-esterification reactor (RTRANS1 in Fig. 1) at 50 °C. Excess methanol is advantageous as trans-esterification is a mass-transfer controlled reaction [26]. So, methanol to oil molar flow ratio of 6 is maintained in each trans-esterification reactor [1,4]. Trans-esterification section mainly contains continuous stirred tank reactors (CSTRs), distillation

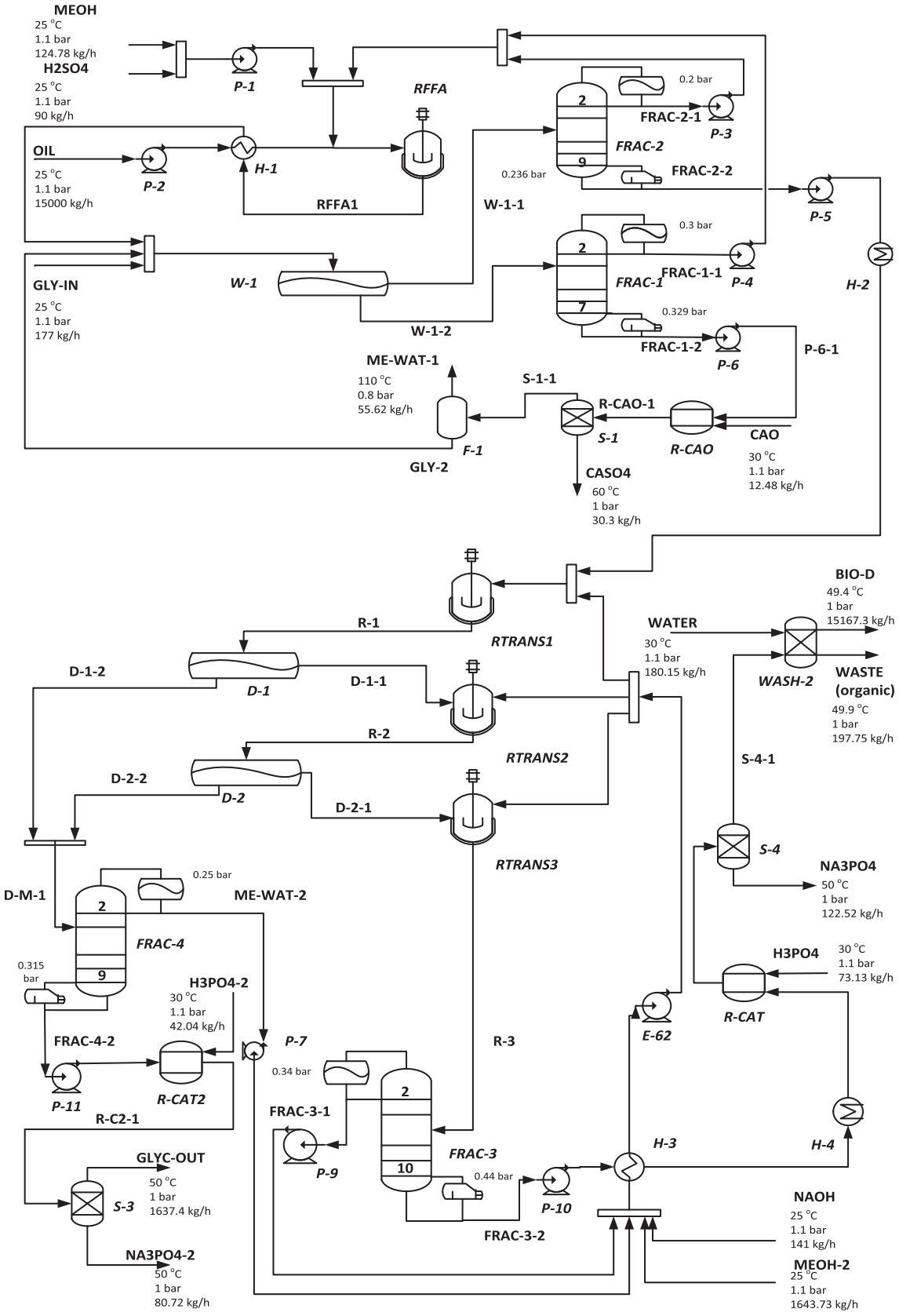

Fig. 1. Biodiesel production process involving esterification (top section) and trans-esterification (bottom section): methanol removal is followed by water washing (Process 1).

columns, phase separators, a neutralization reactor and a washing column. Three CSTRs are placed in series, and treated oil mixed with methanol and NaOH catalyst is charged to the first CSTR (i.e. RTRANS1). The effluent streams from RTRANS1 and RTRANS2 are individually sent to phase separators, where glycerol and NaOH with some methanol are separated as the heavy phase (i.e. streams

'D-1-2' and 'D-2-2'). The light phase (i.e. streams 'D-1-1' and 'D-2-1') from D-1 and D-2 separators goes to RTRANS2 and RTRANS3 reactors, respectively. This phase mainly contains biodiesel, oil and methanol with some NaOH. Finally, stream 'R-3' is charged to a distillation column (FRAC-3) having 11 theoretical stages and operating at reflux ratio of 1, where 98% methanol is recovered and reused in the trans-esterification reactors.

Bottom product from FRAC-3 column contains mainly biodiesel, and is treated in a neutralization unit to remove NaOH using phosphoric acid. A gravity separator 'S-4' is then used to separate precipitated salt from stream 'NA3PO4-2'. It is followed by a water wash column (WASH-2). As the recycled methanol should be free of water, water wash column is used after separating methanol from the reaction mixture. From WASH-2 column, the stream BIO-D containing FAMEs (i.e., Methyl-oleate, Methyl-palmitate, Methyl-myristate, Methyl-stearate, Methyl-linoleate) and having a flow rate of 15167.3 kg/h with more than 99% purity, is taken out. The remaining unreacted oil, methanol, glycerol, etc. are removed from stream 'WASTE' with a flow rate of 197.75 kg/h.

Glycerol streams (i.e. streams 'D-1-2' and 'D-2-2') are mixed together and charged to a distillation column (FRAC-4), where most of the methanol (stream ME-WAT-2) is separated and recycled. The bottom stream (FRAC-4-2) is mainly glycerol and NaOH, and is charged to the neutralization reactor (R-CAT2) to neutralize NaOH present in the streams using phosphoric acid. The Na_3PO_4 formed in the neutralization reactor is separated using the gravity separator (S-3) from stream NA3PO4-2. The top stream 'GLYC-OUT', having more than 96% glycerol, is taken out at a flow rate of 1637.4 kg/h. Fig. 1 shows temperature, pressure and flow rate of all inlet and exit streams of Process 1.

2.2. Process 2

Fig. 2 shows an alternative process, where washing is followed by products separation, used by Morais et al. [1]. The WCO feed of 15,000 kg/h (stream 'OIL' in Fig. 2) is pre-heated in a heat exchanger (H-1) with the esterification reactor products (stream 'RFFA1') and then fed to the esterification reactor (RFFA), where FFAs are converted to FAMEs. Esterification takes place at 60 °C, 4 bar, methanol (stream 'MEOH') to FFAs molar ratio of 10:1 and with 10% (w/w) of sulfuric acid catalyst relative to FFAs. The esterification products (stream 'RFFA1'), after passing through the heat exchanger 'H-1', are charged with glycerol to the 'WASH-1' column, where sulfuric acid and water are separated from the reaction mixture. Glycerol is added to achieve required separation. Here, a wash column 'WASH-1' is used instead of a phase separator 'W-1' in Process 1. The treated oil that leaves the 'WASH-1' column (stream 'WASH-1-1') is sent to the trans-esterification reactor. The other stream from 'WASH-1' column (stream 'WASH-1-2') mainly contains glycerol, methanol, water and acid catalyst, which is then sent to a distillation column (FRAC-1 with 6 theoretical stages and operating at a reflux ratio of 1.1) to recover the unreacted methanol (stream 'FRAC-1-1') for recycling to the esterification reactor (RFFA). Glycerol and sulfuric acid leave the FRAC-1 column in the bottom stream (FRAC-1-2), which is fed to a neutralization reactor (R-CAO) where sulfuric acid reacts with calcium oxide to produce calcium sulphate (stream 'CAO'). The precipitated calcium sulfate is removed in a gravity separator (S-1) and treated as a waste stream (CASO4). The glycerol stream (S-1–1) leaving the separator S-1 is further purified in a flash evaporator (F-1) where the remaining methanol and water are removed in the top stream (ME-WAT-1) and treated as a waste stream due to small methanol flow rate of 14.715 kg/h. Glycerol is then recycled back and mixed with fresh glycerol.

The pretreated oil stream (WASH-1-1 in Fig. 2) from the esterification reactor is then processed in the trans-esterification reactor (RTRANS), where a 6:1 M ratio of methanol to oil is used with 1% (w/w) of NaOH (stream 'NAOH') in oil. Trans-esterification takes place at 50 °C and 4 bar in about 2 h. In addition to the recycled methanol (stream 'FRAC-2-1'), fresh methanol (stream 'MEOH-1') is added to maintain the required ratio of methanol to oil. The anhydrous NaOH is dissolved in fresh methanol. The trans-esterification products (stream 'RTRANS1') goes to the distillation column (FRAC-2 having 10 theoretical stages and operating at a reflux ratio of 1.0), where 98% methanol is recovered as the column top stream 'FRAC-2-1' and recycled back to the trans-esterification reactor. The column bottom stream (FRAC-2-2), mainly containing biodiesel and glycerol, flows through heat exchangers H-2 and H-3, where it is cooled using streams S-3-1 and WASH-2–1 respectively; it is then charged to the WASH-2 column. Methanol, glycerol and catalyst are separated from biodiesel and unreacted oil in 'WASH-2'. The stream WASH-2-1, mainly containing biodiesel and unconverted oil, is then fed to the distillation column (FRAC-3) having 15 theoretical stages and operating at the reflux ratio of 1.0. In FRAC-3, a partial condenser is used to separate methanol and water from stream ME-WAT-3 having a flow rate of 36.04 kg/h, which is not recycled due to its low methanol content (35.6 wt%).

From stream 'FRAC-3-1', biodiesel of more than 99% purity is separated at the rate of 15104.5 kg/h and then used to heat the stream 'H-3-2' in exchanger H-4. Unconverted oil obtained from the bottom stream (FRAC-3-2) at a flow rate of 312.06 kg/h is recycled and mixed with fresh WCO. The bottom stream from the WASH-2 column, containing mainly glycerol (stream WASH-2-2), goes to a neutralization reactor (R-CAT) for removing the catalyst. Phosphoric acid is mixed in equivalent moles to the NaOH present in the stream WASH-2-2.

The resulting salt (i.e. Na_3PO_4) is then removed in a gravity separator (S-3). Glycerol resulting from the neutralization reactor (R-CAT) is further purified in a distillation column (FRAC-4) having 10 theoretical stages and operating at a reflux ratio of 1.1. The top stream (ME-WAT-2), containing mainly methanol and water, is not recycled due its small flow rate and methanol content (11.5 wt%). The bottom stream (FRAC-4–2) is more than 96% pure glycerol by-product at a flow rate of 1628.8 kg/h.

Unlike Process 1 (Fig. 1), a single trans-esterification reactor is used in Process 2. Further, methanol is not recovered from the treated oil in the esterification section. The effluent of trans-esterification reactor (RTRANS1) is sent to the distillation column (FRAC-2), where unreacted methanol is separated. Due the presence of unreacted methanol and alkali catalyst, reversible reactions might take place, which is undesirable. In addition, bottom product of FRAC-2 is fed to the wash column, and then unreacted oil, methanol and products are separated in FRAC-3 and FRAC-4. Due to this, the recovered methanol contains excess water, which makes it undesirable to reuse. Process 2 uses a distillation column (FRAC-3) with partial condenser to remove methanol and water in the vapour phase from stream MET-WAT-3. Fig. 2 shows temperature, pressure and flow rate of all inlet and exit streams of Process 2.

3. Process simulation and multi-objective optimization

This section discusses the simulation of the two alternate biodiesel processes in Aspen Plus followed by MOO using NSGA-II.

3.1. Process simulation

The biodiesel production processes using WCO (shown in Figs. 1 and 2) have been simulated in the Aspen Plus V-8. The palm oil is a mixture of triglycerides of oleic, linoleic, myristic, palmitic, stearic and other acids. Unlike many earlier studies, detailed composition

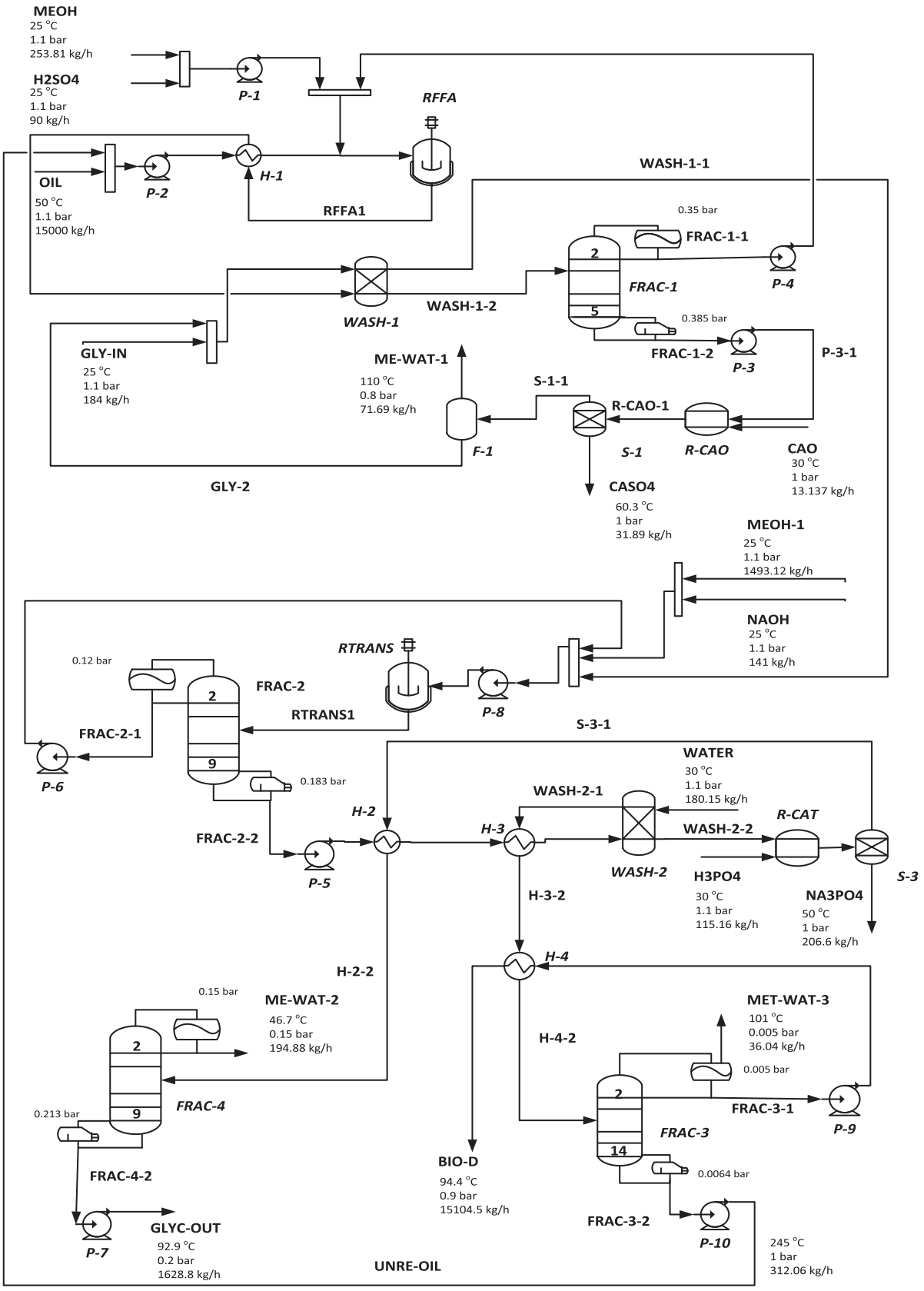

Fig. 2. Biodiesel production process involving esterification (top section) and trans-esterification (bottom section): water washing is followed by products separation (Process 2).

of palm oil is considered in this study. As the detailed composition of waste cooking palm oil is not available in the literature, the detailed composition of refined, bleached and deodorized (RBD) palm oil is taken from [27,28], and adjusted to include 6 percent FFAs. The detailed fatty acid distribution in diglycerides (DG) is not given. Therefore, all the diglycerides in the feed are represented as the PP molecule (see Table S1 in the Supplementary Data). DG such as 1-3-dimyristin, 1-3-dipalmitin, 1-3-diolein and monoglycerides (MG) including 1-monomyristin, 1-monopalmitin, 1-monostearin, 1-monoolein and 1-monolinolein are the intermediates of the trans-esterification reaction. Methyl-oleate, Methyl-palmitate, Methyl-myristate, Methyl-stearate and Methyl-linoleate are the biodiesel products. Table S1 in the Supplementary Data lists the detailed glyceride and FFA compositions in the WCO feed. NaOH is used as the catalyst, and is removed by adding H_3PO_4 to precipitate Na_3PO_4. As the electrolyte chemistry is not modeled in detail, these electrolytes are simulated using physical property data for water, but considering their correct molecular weights [28].

In this study, detailed kinetics including intermediate mono- and di-glycerides formation, are considered for obtaining realistic results. Physical properties of mono-, di- and tri-glycerides are taken from the Aspen Plus database. Esterification and trans-esterification kinetics used are respectively taken from [25] and [28]. The trans-esterification kinetics in [28] were extracted from Narvaez et al. [29], who reported them for palm oil and not for the individual triglycerides present. Therefore, reaction kinetics of all the constituent triglycerides were assumed to be the same as that for the triglyceride mixture in palm oil. For example, both reactions 1–7 (see reaction set S2 in Supplementary Data) produce diglycerides (DG) from triglycerides (TG), and hence their rate constants are considered as equal [28]. Note that the uncertainty in the kinetics may have some effect on the calculations, but this effect will not influence the results significantly. The property model used for biodiesel process simulation is Dortmund modified UNIFAC as researchers [2,21,28,30] successfully used this model to predict the physical properties of the considered components. Redlich–Kwong–Soave equation of state (RKS EOS) is used to predict the physical properties of the vapor phase. Thermophysical property model parameters of tri-, di-, and mono-glycerides such as vapour pressure, heat of vaporization, heat of formation, heat capacity, liquid molar volume and liquid viscosity are taken from biodiesel databank of Aspen Plus. The detailed information for the development of these thermophysical property models has been presented in [31–33]. In addition, the required T_C, P_C and ω (critical temperature, critical pressure and acentric factor) for RKS EOS are estimated with the Gani group contribution method [28]. Although the experimental or industrial validation could not be carried, the simulated results such as conversion in esterification and trans-esterification section, and product quality have been found in agreement with the literature data [16,22].

A fixed pressure of 4 bar is assumed in both esterification and trans-esterification reactors while reactor temperatures are considered as decision variables in the optimization. In both the process alternatives, product purities were defined to be 99% (w/w) for biodiesel, which is higher than the European biodiesel standard (EN 14214) specification for esters content (i.e., 96.5% w/w). Vacuum operation for methanol recovery and products purification is employed for maintaining the temperatures at suitably low levels to avoid the thermal decomposition of biodiesel (<523.15 K) and glycerol (<423.15 K) [1,28]. Further, atmospheric pressure is assumed in neutralization reactors and water wash columns.

3.2. Multi-objective optimization

Both the biodiesel processes were optimized for profit, heat duty and organic waste. Methanol, glycerol, tri/di/mono-glycerides, FAMEs and FFAs in stream 'WASTE' and methanol in stream 'ME-WAT-1' in Fig. 1, are considered as the constituents of organic waste in Process 1. Methanol in streams 'ME-WAT-1', 'ME-WAT-2', and 'ME-WAT-3' in Fig. 2, is considered as organic waste in Process 2. The effect of these different definitions of organic waste is discussed in Sections 4.1.2 and 4.2.2. Profit is calculated by subtracting cost of manufacture (COM) from the revenue obtained by selling the products: biodiesel and glycerol. Table S3 in the Supplementary Data presents the cost of raw materials, products and utilities, used in the present study.

As described in Section 2, potential WCO is 120 kt/annum (equivalent to 15000 kg/h). Given the uncertainty in the WCO availability, this work considers −20% variation in WCO as one of the decision

Table 1
Different optimization cases studied for biodiesel production processes.

Objective function	Decision variables	Constraints
Processes 1 and 2	Process 1	Process 1
Case A:	$96 \leqslant$ WCO $\leqslant 120$ kt/annum	Mass purity: $x_{Biodiesel} \geqslant 0.99$
Max. Profit (million USD/annum)	$55 \leqslant T_{RFFA} \leqslant 65$ °C	Mass purity: $x_{Glycerol} \geqslant 0.95$
Min. Heat duty (MW)	$45 \leqslant T_{RTRANS1} \leqslant 60$ °C	(Methanol Recovery)$_{FRAC\text{-}1,\ FRAC\text{-}3,\ FRAC\text{-}3,\ FRAC\text{-}4} \geqslant 0.98$
Case B:	$45 \leqslant T_{RTRANS2} \leqslant 60$ °C	$T_{FRAC\text{-}1} \leqslant 150$ °C
Max. Profit (million USD/annum)	$45 \leqslant T_{RTRANS3} \leqslant 60$ °C	$T_{FRAC\text{-}2} \leqslant 150$ °C
Min. Organic waste (tons/annum)	1.5 $\leqslant$ (Residence Time)$_{RFFA} \leqslant$ 2.5 h	$T_{FRAC\text{-}3} \leqslant 250$ °C
	1.5 $\leqslant$ (Residence Time)$_{RTRANS1} \leqslant$ 2.5 h	$T_{FRAC\text{-}4} \leqslant 150$ °C
	1.5 $\leqslant$ (Residence Time)$_{RTRANS2} \leqslant$ 2.5 h	
	1.5 $\leqslant$ (Residence Time)$_{RTRANS3} \leqslant$ 2.5 h	
	$2 \leqslant$ (Feed Stage)$_{FRAC\text{-}1} \leqslant 7$	
	$2 \leqslant$ (Feed Stage)$_{FRAC\text{-}2} \leqslant 9$	
	$2 \leqslant$ (Feed Stage)$_{FRAC\text{-}3} \leqslant 10$	
	$2 \leqslant$ (Feed Stage)$_{FRAC\text{-}4} \leqslant 9$	
	Process 2	Process 2
	$96 \leqslant$ WCO $\leqslant 120$ kt/annum	Mass purity: $x_{Biodiesel} \geqslant 0.99$
	$50 \leqslant T_{RFFA} \leqslant 65$ °C	Mass purity: $x_{Glycerol} \geqslant 0.95$
	$45 \leqslant T_{RTRANS} \leqslant 60$ °C	(Methanol Recovery)$_{FRAC\text{-}1,\ FRAC\text{-}3,\ FRAC\text{-}3,\ FRAC\text{-}4} \geqslant 0.98$
	1.5 $\leqslant$ (Residence Time)$_{RFFA} \leqslant$ 2.5 h	$T_{FRAC\text{-}1} \leqslant 150$ °C
	1.5 $\leqslant$ (Residence Time)$_{RTRANS1} \leqslant$ 2.5 h	$T_{FRAC\text{-}2} \leqslant 250$ °C
	$2 \leqslant$ (Feed Stage)$_{FRAC\text{-}1} \leqslant 5$	$T_{FRAC\text{-}3} \leqslant 250$ °C
	$2 \leqslant$ (Feed Stage)$_{FRAC\text{-}2} \leqslant 9$	$T_{FRAC\text{-}4} \leqslant 150$ °C

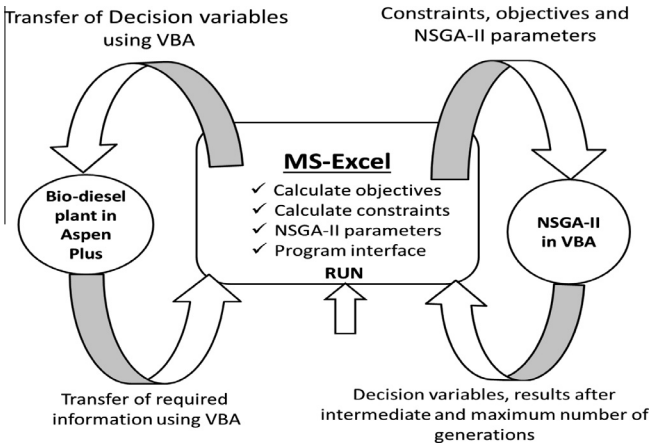

Fig. 3. Framework for EMOO.

variables. Temperature and residence time of each of the CSTRs are also taken as decision variables for optimization as these are very important for the conversion of WCO to biodiesel. Also, feed stage of all distillation columns is taken as a decision variable as it can minimize energy requirement by reducing reboiler duty. In this study, product purities are treated as constraints as these have to be satisfied as per standards. To prevent product deterioration, upper limits for temperatures at the bottom of all distillation columns is considered as additional constraints [16]. MOO for both processes is carried out for two different cases: (1) profit and heat duty, and (2) profit and organic waste. Table 1 provides details on these cases considered in this study. Equipment purchase cost (C_p) and bare module factor (F_{BM}) are calculated based on the correlations and data given in [34]. Total module cost (C_{TM}) and gross roots cost (C_{GR}), which is considered as fixed capital investment (FCI), are calculated using Eqs. (2) and (3), respectively. If the distillation column diameter is less than 0.9 m, then the column is considered to be a packed column; otherwise, trays are assumed in the column [16]. All equipments processing acids are assumed to be built of stainless steel, while all other equipments are assumed to be made of carbon steel. Bare module cost (C_{BM}) is calculated using Eq. (1). Bare module cost at base conditions (C^0_{BM}) denotes the cost when pressure is ambient and carbon steel is the material of construction.

$$C_{BM} = \sum_{\text{all equipments}} C_p F_{BM} \tag{1}$$

$$C_{TM} = 1.18 C_{BM} \tag{2}$$

$$\text{FCI or } C_{GR} = C_{Tm} + 0.50 \sum_{\text{all equipments}} C^0_{BM} \tag{3}$$

The operating labor cost is calculated based on the procedure given in Turton et al. [35]. COM and then profit are calculated using the following equations [35].

$$\text{COM} = 0.28(\text{FCI}) + 2.73(\text{operating labor cost}) + 1.23(\text{cost of utilities} + \text{cost of raw material}) \tag{4}$$

$$\text{Profit} = \text{Revenue} - \text{COM} \tag{5}$$

In this study, an Excel-based MOO (EMOO) program [36], which is based on the binary-coded NSGA-II, has been used for determining the optimal trade-offs between different objectives. In this

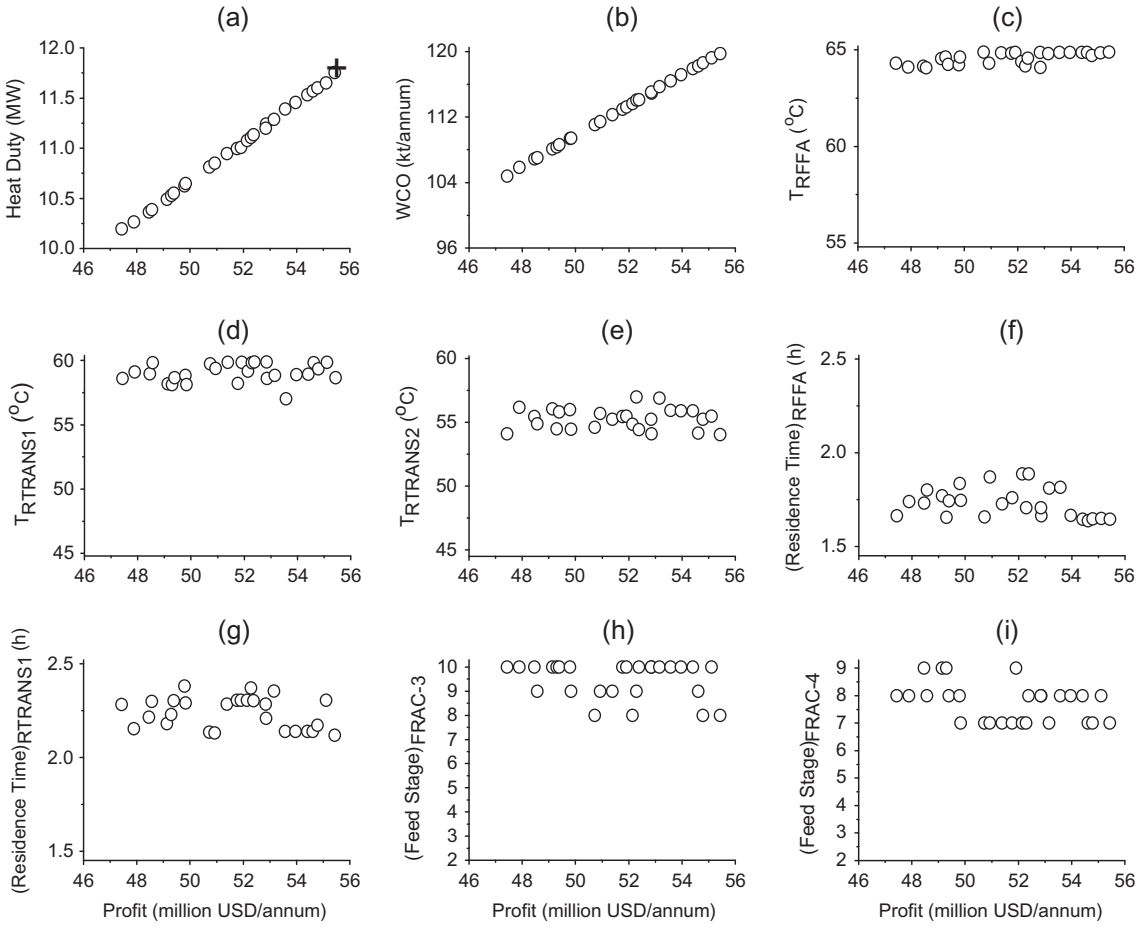

Fig. 4. Simultaneous maximization of profit and minimization of heat duty for Process 1.

program, objective functions and constraints are computed in Excel worksheets, whereas NSGA-II is executed inside the Excel Macro (Visual Basic for Applications). The algorithm used in the EMOO program is described in [36]. Values of NSGA-II parameters used for all optimization cases in this work are: population size (NP) = 100, two-point crossover with probability = 0.9, mutation probability = 0.05, random seed = 0.5, and maximum number of generations = 100.

In this work, the EMOO program is interfaced with Aspen Plus using visual basic application (VBA) (Fig. 3). NSGA-II in this program generates a set of decision variables values (Table 1), and these values are sent to the Aspen Plus simulator.

The simulation is converged for each set of values of decision variables, and required results from Aspen Plus simulation (such as flow rates, mass fractions and utilities) are sent to the EMOO program. In Excel, these results are used to determine the values of objective functions and constraints, which are in turn used by NSGA-II. Then, NSGA-II generates another set of values for decision variables, and the above procedure is repeated. The iterative calculations continue until the specified stopping criterion is satisfied.

4. Results and discussion

4.1. Pareto-optimal solutions for Process 1

4.1.1. Case 1: Trade-off between profit and heat duty

The optimal trade-off between profit and heat duty for Process 1 is shown in Fig. 4a. All the solutions on the Pareto-optimal front are equally good for the objectives used, and any solution can be selected based on engineer's preference and other requirements.

The increase in annual profit from 47.45 to 55.44 million USD requires a proportional increase in heat duty from 10.20 to 11.75 MW (Fig. 4a). This is mainly due to the increased WCO from 104.76 to 119.73 kt/annum (Fig. 4b). The temperatures of esterification reactor 'T_{RFFA}' (Fig. 4c), trans-esterification reactor '$T_{RTRANS1}$' (Fig. 4d) and trans-esterification reactor '$T_{RTRANS3}$' (not shown in Fig. 4 for brevity; see Fig. S1(a) in the Supplementary Data) stay near to their upper bounds. Further, $T_{RTRANS2}$ (Fig. 4e) varies around 55 °C. These higher reactor temperatures lead to better conversion and consequently higher profit. However, this increases the size and so cost of phase-separators 'W-1', 'D-1' and 'D-2' resulting in higher FCI. Optimal residence time in esterification reactor '(Residence Time)$_{RFFA}$' (Fig. 4f) is largely scattered between 1.6 and 1.9 h. This suggests that smaller reactor volume smaller residence time: 1.6–1.9 h) with higher temperature is sufficient to achieve the required conversion of the FFAs to biodiesel. Optimal residence times in trans-esterification reactors: '(Residence Time)$_{RTRANS1}$' (Fig. 4g), '(Residence Time)$_{RTRANS2}$' (Fig. S1(b) in the Supplementary data) and '(Residence Time)$_{RTRANS3}$' (Fig. S1(c)) are largely scattered near to their upper bounds. These are required to obtain optimum conversion of WCO, though larger reactor volumes increase the capital cost. In general, optimum feed stages for columns 'FRAC-1' (Fig. S1(d)), 'FRAC-2' (Fig. S1(e)), 'FRAC-3' (Fig. 4h) and 'FRAC-4' (Fig. 4i) are scattered towards their upper bounds. These do not have much impact on FCI, but increases the profit by reducing the utility cost for the column reboiler and condenser. Pareto-optimal solution (shown as + in Fig. 4a) is considered for further discussion in the Section 4.3. Table S4 in the

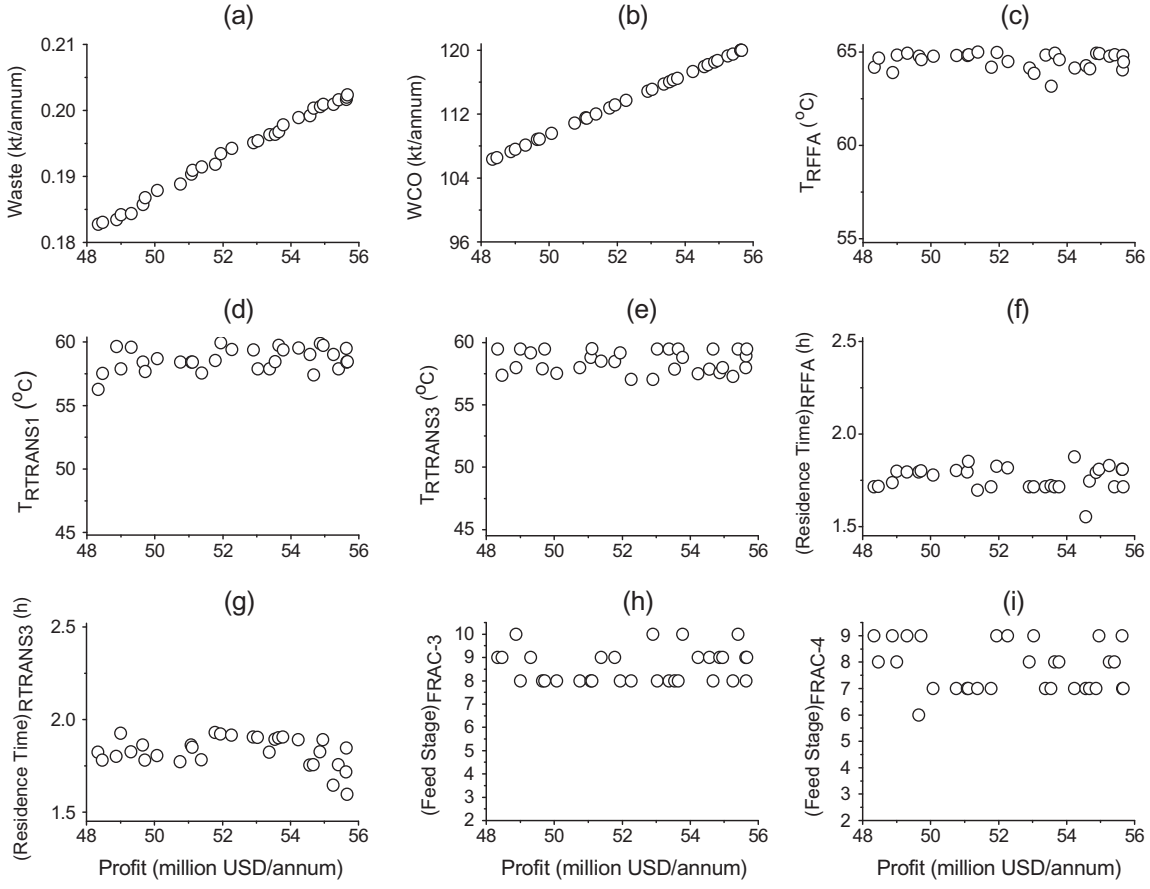

Fig. 5. Simultaneous maximization of profit and minimization of organic waste for Process 1.

Supplementary Data presents the key data of selected streams corresponding to this optimal solution.

4.1.2. Case 2: Trade-off between profit and organic waste

Fig. 5a presents Pareto-optimal front obtained for maximizing profit and minimizing organic waste. Organic waste increases from 0.183 to 0.202 kt/annum for the profit improvement from 48.32 to 55.68 million USD per annum. Methanol, glycerol, tri/di/mono-glycerides, FFAs and FAMEs are the constituents of organic waste. As the waste stream ('WASTE' in Fig. 1) contains glycerol and FAME, minimization of organic waste improves the profit to some extent. In general, the main decision variable affecting the profit and organic waste is the amount of WCO processed (Fig. 5). Higher values of T_{RFFA}, $T_{RTRANS1}$, $T_{RTRANS3}$ (Fig. 5b–e) also improve the profit as larger amount of biodiesel is produced from WCO in smaller reactors at higher temperatures. As $T_{RTRANS2}$ stays near to its lower bound of 45 °C (Fig. S2(a) in the Supplementary Data), higher temperature is required in $T_{RTRANS3}$ to convert the remaining oil to FAME (Fig. 5e).

Lower $T_{RTRANS2}$ favors the profit by reducing the cost of phase separator 'D-2'. As higher temperatures of reactors favor both objectives similarly, most of the decision variables related to the temperature are closer to their upper bounds. However, this leads to increase in FCI as larger phase separators are required to achieve sufficient separation. Optimal residence time of esterification reactor: '$(\text{Residence Time})_{RFFA}$' (Fig. 5f) is largely scattered between 1.5 and 1.88 h, which suggests that smaller reactor operating at higher temperature is better to achieve the required conversion of FFAs to FAME. Optimal residence times of first two trans-esterification reactors are largely scattered towards their upper bounds (Figs. S2(b) and S2(c)); $(\text{Residence Time})_{RTRANS3}$ (Fig. 5g) is scattered between 1.6 and 1.93 h. These are required to obtain optimum conversion of WCO to FAME, which increases the profit and also reduces amount of organic waste. The optimum feed stages for columns 'FRAC-1' (Fig. S2(d)), 'FRAC-2' (Fig. S2(e)), 'FRAC-3' (Fig. 5h) and 'FRAC-4' (Fig. 5i) are scattered towards their upper bounds, which are the stages close to the reboiler. Although these do not affect the generation of organic waste, they increase the profit by reducing the energy requirements of the columns.

4.2. Pareto-optimal solutions for Process 2

4.2.1. Case 1: Trade-off between profit and heat duty

The trade-off between profit and heat duty for Process 2 in Fig. 6a is similar to that for Process 1.

The profit improves from 44.30 to 54.57 million USD per annum as heat duty increases proportionately from 13.71 to 16.36 MW. As opposed to Process 1, Process 2 has no intermediate phase separators, whose cost would vary as a result of variation in the reactor temperature. In both the processes, larger profit can obtained at higher capacity, but this also increases the heat duty. As expected, increase in heat duty and profit (Fig. 6a) is mainly due to the increased WCO from 97.13 to 118.02 kt/annum (Fig. 6b). Initially, esterification reactor temperature, 'T_{RFFA}' (Fig. 6c) stays near to its upper bound. Later, it is scattered between 61.9 and 65 °C (Fig. 6c). Trans-esterification reactor temperature, 'T_{RTRANS}' is scattered between 52 and 60 °C, especially in the later part (Fig. 6d). Higher profit is obtained as better conversion of WCO to FAME is achieved at higher temperatures. The residence time of esterification reactor '$(\text{Residence Time})_{RFFA}$' increases from 1.54 to 2.5 h,

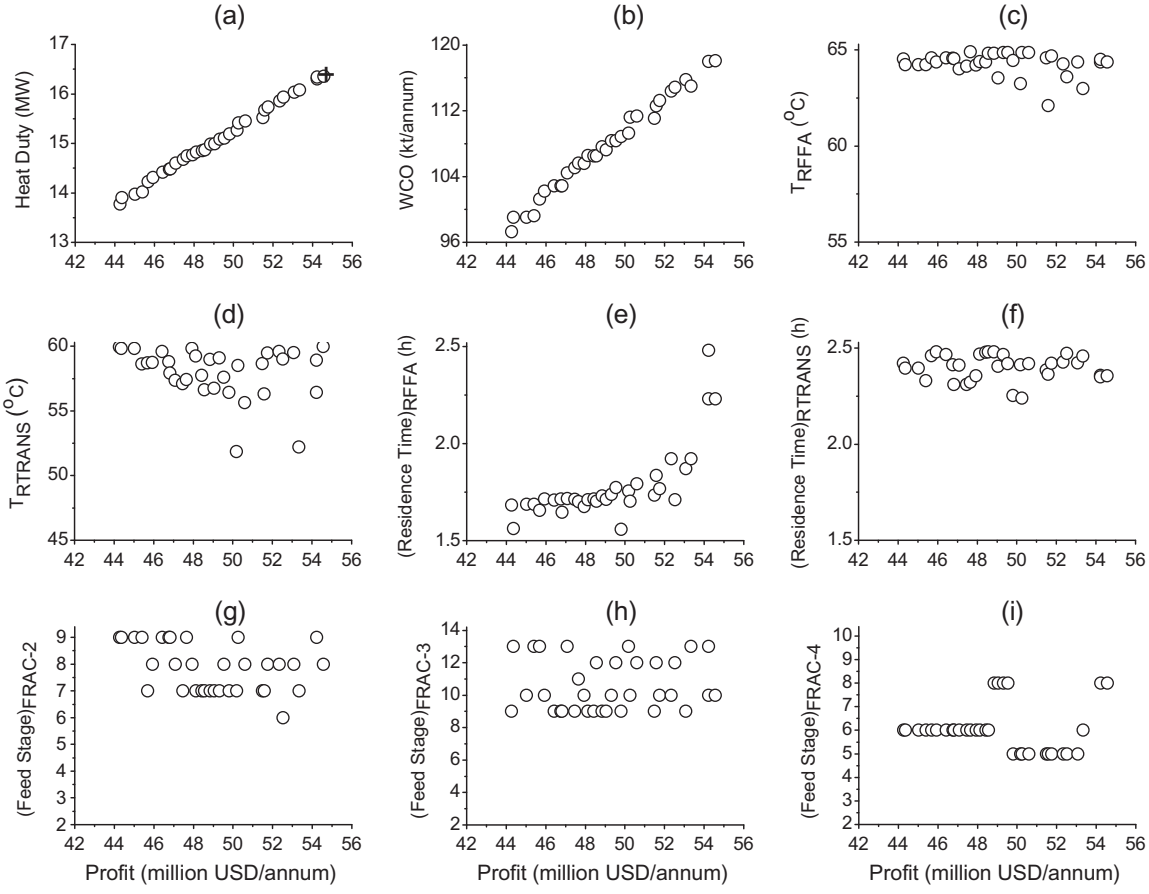

Fig. 6. Simultaneous maximization of profit and minimization of heat duty for Process 2.

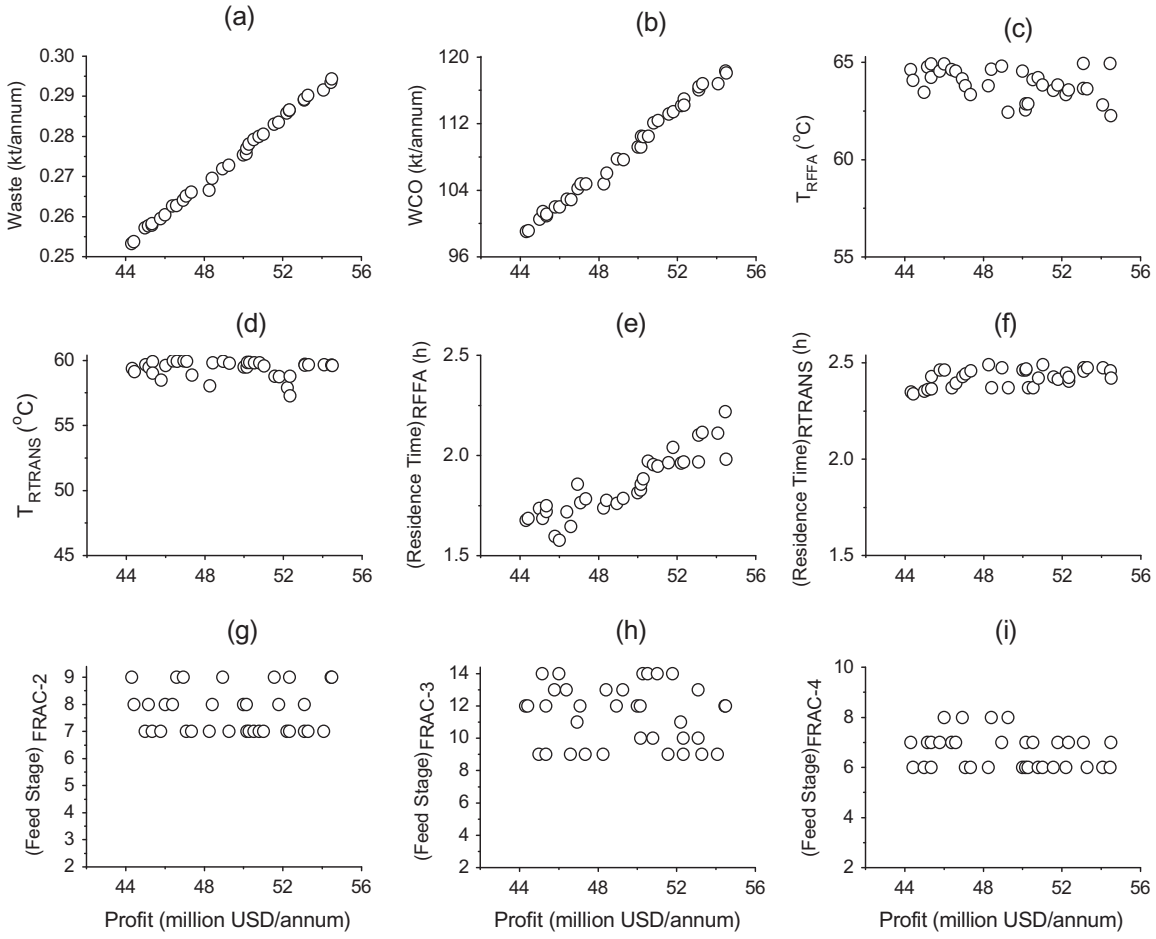

Fig. 7. Simultaneous maximization of profit and minimization of organic waste for Process 2.

Table 2
Comparison of Processes 1 and 2 (corresponding to the optimal solution + in Figs. 4a and 6a).

Quantity	Process 1 A	Process 2 B	% Difference (A–B) × 100/A
FCI or C_{GR} (million USD)	12.95	12.73	1.70
Methanol flow rate (kt/annum)	14.12	13.76	2.55
Biodiesel produced (kt/annum)	121.09	118.95	1.77
COM (million USD/annum)	73.5	72.8	0.95
Organic waste (kt/annum)	0.221	0.292	−32.13
Heat Duty (MW)	11.75	16.36	−39.23
Profit (million USD/annum)	55.44	54.57	1.57

Table 3
Comparison of biodiesel quality specifications for the optimal solutions of Processes 1 and 2 (shown as + in Figs. 4a and 6a) with those required by EN14214.

Parameters	Process 1 (detailed components)	Process 1 (lumped component)	Process 2 (detailed components)	EN14214 [38]
Methyl-O (wt%)	38.01	99.12	36.72	–
Methyl-P (wt%)	48.79	0.0	47.59	–
Methyl-M (wt%)	2.10	0.0	3.20	–
Methyl-S (wt%)	2.70	0.0	3.79	–
Methyl-Li (wt%)	7.69	0.0	8.20	–
Biodiesel (= sum of above) (wt%)	99.29	99.12	99.5	>96.5
Monoglycerides (ppm)	286	292	251	<8000
Diglycerides (ppm)	99	103	83	<2000
Triglycerides (ppm)	112	115	99	<2000
Glycerol (ppm)	Trace	Trace	Trace	<2500
Methanol (ppm)	608	539	316	<2000
Density (15 °C) (kg/m^3)	869.42	861.63	866.167	860–900

particularly at high profit (Fig. 6e). This is required to obtain sufficient conversion of FFAs to FAME. Optimal residence time of trans-esterification reactor '(Residence Time)$_{RTRANS}$' (Fig. 6f) is scattered between 2.24 and 2.5 h. Capital cost increases with reactor size, but large reactor is required to obtain optimum conversion of WCO. Trans-esterification reactor design is very critical as this process has only one reactor unlike in Process 1, which has three trans-esterification reactors in series. In general, optimum feed stages for columns 'FRAC-1' (Fig. S3 in the Supplementary Data), 'FRAC-2' (Fig. 6g), 'FRAC-3' (Fig. 6h) and 'FRAC-4' (Fig. 6i) are scattered towards their upper bounds, which increase the profit by reducing the utility cost in reboilers and condensers. The optimal solution, shown as + in Fig. 6a, is taken for further analysis in Section 4.3. Table S5 in the Supplementary Data presents the key data of selected streams corresponding to this optimal solution.

4.2.2. Case 2: Trade-off between profit and organic waste

Fig. 7a presents the Pareto-optimal solutions obtained for simultaneous maximization of profit and minimization of organic waste for Process 2. Organic waste increases from 0.253 to 0.295 kt/annum for the improvement in profit from 44.15 to 54.50 million USD per annum. These increases are mainly due to the increased WCO from 98.98 to 118.35 kt/annum (Fig. 7b). Note that only methanol in streams: 'ME-WAT-1', 'ME-WAT-2' and 'ME-WAT-3' in Fig. 2, is the organic waste in Process 2, which does not affect profit much. Optimal values of T_{RFFA} and T_{RTRANS} are near to their upper bounds of 65 and 60 °C, respectively (Fig. 7c and d), which improve the profit by maximizing the product formation. Optimal (Residence Time)$_{RFFA}$ increases from 1.55 to 2.23 h, which is required to convert FFAs into FAME (Fig. 7e). Optimal (Residence Time)$_{RTRANS}$ is near to its upper bound (scattered between 2.32 and 2.5 h), for converting most of the oil into FAME (Fig. 7e); this has favorable impact on the profit without affecting the organic waste. Optimum feed stages for columns 'FRAC-1' (Fig. S4 in the Supplementary Data), 'FRAC-2' (Fig. 7g), 'FRAC-3' (Fig. 7h) and 'FRAC-4' (Fig. 7i) are scattered towards their upper bounds, which increase the profit by reducing the utility cost in reboilers and condensers of different columns. Similar to Process 1, they do not affect the generation of organic waste but improve the profit by reducing COM.

4.3. Comparison of Processes 1 and 2 for their economic merit and environmental impact

Table 2 compares several quantities for the selected optimal solutions for Processes 1 and 2 (represented by + in Fig. 4a and Fig. 6a, respectively). Although all the solutions on the Pareto-optimal front are equally good, the optimal solution corresponding to the highest profit for each process is chosen for a fair comparison. West et al. [10] reported C_{TM} of 1.1 million USD (when CEPCI = 394) for a biodiesel plant of capacity 8 kt/annum with WCO as the feed-stock. Further, Sharma and Rangaiah [16] reported C_{TM} of 2.88 million USD (for CPECI = 600) for a biodiesel plant of capacity 20 kt/annum with WCO as the feed-stock. Projected C_{TM} for a plant capacity of 120 kt/annum, using the six-tenths rule [34], and CEPCI of 600, is 8.44 million USD (based on [16]) and 8.5 million USD (based on [10]). In the present study, C_{TM} of 9.31 million USD for Process 1 and 9.30 million USD for Process 2 are obtained, and these are consistent with the previous studies. The small increase in C_{TM} is mainly due to the increased number of processing steps in both the processes (see Figs. 1 and 2). Apostolakou et al. [37] reported FCI of 9.4 million USD for the biodiesel plant having capacity of 50 kt/annum; this is due to the different procedure used for FCI calculation.

From Table 2, it can be seen that FCI for Process 1 is slightly higher than that for Process 2, mainly due to the more number of equipments involved in the former process. Amount of methanol required in Process 1 is slightly higher than that of Process 2, mainly due to slightly larger WCO in Process 1. As water wash column is placed after methanol recovery column in Process 1, recovered methanol is almost free from water. This leads to less energy-intensive methanol recovery. COM for Process 1 is marginally higher than that of Process 2, mainly due to higher FCI in Process 1. Amount of organic waste generated in Process 1 is significantly lower (32%) than that in Process 2. Also, heat duty of Process 1 is significantly lower (39%) than that of Process 2. Lower heat duty and lower organic waste suggest that Process 1 has lower environmental impact compared to Process 2.

Further, the present study reveals that, despite more number of equipments involved, Process 1 is slightly more profitable than Process 2. This is mainly due to reduced utility cost and increased revenue resulting from the increased product formation (Table 2); these in turn are attributed to the processing sequence with three CSTRs in series, where intermediate phase separators are used to remove heavy phase and prevent backward reactions. Moreover, in Process 1, biodiesel and glycerol are separated first followed by methanol separation and washing of biodiesel. The advantages of this scheme include: (1) it prevents backward reactions as methanol is not removed until separation between biodiesel and glycerol is complete, and (2) as water washing is carried out after methanol removal, the recovered methanol contains very small fraction of water, which avoids energy intensive methanol–water separation and enables methanol re-use in the process. Comparative results in Table 2 for the optimized process alternatives are consistent with Myint and El-Halwagi [12], who concluded that the best flow-sheet is with the biodiesel and glycerol separation first, followed by methanol recovery and finally water washing.

Finally, properties of biodiesel obtained from Aspen Plus simulation, are analyzed to evaluate the quality of biodiesel, and then it is compared against EN standards (European Norms: European standards that describe the requirements and test methods for biodiesel). The results presented in Table 3 show that the quality of the produced biodiesel meets the minimum required standards. To investigate the effect of using detailed composition of oil versus lumped component, optimized Process 1 was simulated with all triglycerides lumped into triolein and all FFAs lumped into oleic acid. Total heating load (Q_H), which is the sum of heating required in reboilers, reactors and heaters, is compared for these two cases. It is found to be 5.61 MW when detailed oil components are used, compared to Q_H of 5.71 MW when the oil components are lumped together. The quality of biodiesel is also analyzed for these two cases. As expected, the constituent methyl esters considering detailed and lumped oil components are different; consequently, quality (such as density) of the biodiesel products is different (Table 3). Although no practical validation is carried out, differences in the results indicate that more details, as used in this study, should be considered for more realistic simulation and optimization.

5. Conclusions

In this study, two alternative alkali-catalyzed biodiesel production processes are simulated in Aspen Plus, considering detailed reaction kinetics and detailed constituents of oil. These processes use waste cooking palm oil as the feed, which is favorable from the point of both economic feasibility and environmental impact. Two bi-objective problems are solved using EMOO program incorporating NSGA-II, to investigate the performance of both the process alternatives. Trade-offs between profit and heat duty, and profit and organic waste are analyzed, which examine profitability and environmental impact of biodiesel processes. Improvement in the profit is accompanied by increase in heat duty, and also with

increased formation of organic waste. The main contributor to these increases is WCO flow rate. Process 1 is found to have a significantly lower organic waste (by 32%), lower heat duty requirement (by 39%) and slightly more profit (by 1.6%), as compared to Process 2. Also, the effect of using detailed components of oil versus lumped component is analyzed and found to have some impact. Hence, considering detailed composition of oil with detailed reaction kinetics is recommended for biodiesel process simulation, for obtaining more realistic results.

Acknowledgement

The authors gratefully acknowledge Universiti Sains Malaysia for the financial support (RU grant: 1001/PJKIMIA/814155).

Appendix A. Supplementary material

Supplementary data associated with this article can be found, in the online version, at http://dx.doi.org/10.1016/j.enconman.2014.05.034.

References

[1] Morais S, Mata TM, Martins AA, Pinto GA, Costa CAV. Simulation and life cycle assessment of process design alternatives for biodiesel production from waste vegetable oils. J Clean Prod 2010;18(13):1251–9.
[2] Patle DS, Ahmad Z. Techno-economic analysis of an alkali catalyzed biodiesel production using waste palm oil. Appl Mech Mater 2014;465–466:120–4.
[3] Canakci M. The potential of restaurant waste lipids as biodiesel feedstocks. Bioresource Technol 2007;98(1):183–90.
[4] Freedman B, Pryde EH, Mounts TL. Variables affecting the yields of fatty esters from transesterified vegetable oils. J Am Oil Chem Soc 1984;61:1638–43.
[5] Ma F, Clements LD, Hana MA. The effects of catalyst, free fatty acids and water on transesterification of beef tallow. T ASAE 1998;41:1261–4.
[6] Gerpen JV. Biodiesel processing and production. Fuel Process Technol 2005;86(10):1007–97.
[7] Canakci M, Van Gerpen J. Biodiesel production from oils and fats with high free fatty acids. T ASAE 2001;44(6):1429–36.
[8] Zhang Y, Dubé MA, McLean DD, Kates M. Biodiesel production from waste cooking oil: 1. Process design and technological assessment. Bioresource Technol 2003;89(1):1–16.
[9] Zhang Y, Dubé MA, McLean DD, Kates M. Biodiesel production from waste cooking oil: 2. Economic assessment and sensitivity analysis. Bioresource Technol 2003;90(3):229–40.
[10] West AH, Posarac D, Ellis N. Assessment of four biodiesel production processes using HYSYS. Plant. Bioresource Technol 2008;99(14):6587–601.
[11] Talebian-Kiakalaieh A, Amin NAS, Mazaheri H. A review on novel processes of biodiesel production from waste cooking oil. Appl Energy 2013;104:683–710.
[12] Myint L, El-Halwagi M. Process analysis and optimization of biodiesel production from soybean oil. Clean Technol Environ Policy 2009;11(3):263–76.
[13] Nicola GD, Moglie M, Pacetti M, Santori G. Bioenergy II modeling and multiobjective optimization of different biodiesel production processes. Int J Chem React Eng 2010;8(1):12–8.
[14] Martín M, Grossmann IE. Simultaneous optimization and heat integration for biodiesel production from cooking oil and algae. Ind Eng Chem Res 2012;51(23):7998–8014.
[15] Huerga IR, Zanuttini MS, Gross MS, Querini CA. Biodiesel production from *Jatropha curcas*: integrated process optimization. Energy Convers Manage 2014;80:1–9.
[16] Sharma S, Rangaiah GP. Multi-objective optimization of a biodiesel production process. Fuel 2013;103:269–77.
[17] Fauzi AHM, Amin NAS. Optimization of oleic acid esterification catalyzed by ionic liquid for green biodiesel synthesis. Energ Convers Manage 2013;76:818–27.
[18] Rahimi M, Aghel B, Alitabar M, Sepahvand A, Ghasempour HR. Optimization of biodiesel production from soybean oil in a microreactor. Energ Convers Manage 2014;79:599–605.
[19] Ong HC, Masjuki HH, Mahlia TMI, Silitonga AS, Chong WT, Leong KY. Optimization of biodiesel production and engine performance from high free fatty acid *Calophyllum inophyllum* oil in CI diesel engine. Energ Convers Manage 2014;81:30–40.
[20] West AH, Posarac D, Ellis N. Simulation, case studies and optimization of a biodiesel process with a solid acid catalyst. Int J Chem Reac Eng 2007;5. Article A37.
[21] Kiss AA, Segovia-Hernández JG, Bildea CS, Miranda-Galindo EY, Hernández S. Reactive DWC leading the way to FAME and fortune. Fuel 2012;95:352–9.
[22] García M, Gonzalo A, Sánchez JL, Arauzo J, Peña JÁ. Prediction of normalized biodiesel properties by simulation of multiple feedstock blends. Bioresource Technol 2010;101(12):4431–9.
[23] <http://www.lurgi.com/website/Biodiesel.57.0.html?&L=1> [accessed September 2013].
[24] <http://www.platinumgroup.com. my> [accessed September 2013].
[25] Berrios M, Siles J, Martín MA, Martín A. A kinetic study of the esterification of free fatty acids (FFA) in sunflower oil. Fuel 2007;86(15):2383–8.
[26] Noureddini H, Zhu D. Kinetics of transesterification of soybean oil. Biocatal Art 1997;74(11):1457–63.
[27] Man YBC, Haryati T, Ghazali HM, Asbi BA. Composition and thermal profile of crude palm oil and its products. J Am Oil Chem Soc 1999;76:237–42.
[28] Aspen Technology. Aspen Plus – Aspen plus biodiesel model (Examples). 2012.
[29] Narvaez PC, Rincon SM, Sanchez FJ. Kinetics of palm oil methanolysis. J Am Oil Chem Soc 2007;84:971–7.
[30] Kiss AA. Biodiesel by Reactive Absorption – Towards green technologies. In: Jeżowski J, Thullie J, editors. Computer aided chemical engineering: Elsevier; 2009. p. 847–52.
[31] Zong L, Ramanathan S, Chen CC. Fragment-based approach for estimating thermophysical properties of fats and vegetable oils for modeling biodiesel production processes. Ind Eng Chem Res 2010;49:876–86.
[32] Zong L, Ramanathan S, Chen CC. Correction to fragment-based approach for estimating thermophysical properties of fats and vegetable oils for modeling biodiesel production processes. Ind Eng Chem Res 2010;49:3022–3.
[33] Zong L, Ramanathan S, Chen CC. Predicting thermophysical properties of mono- and diglycerides with the chemical constituent fragment approach. Ind Eng Chem Res 2010;49:5479–84.
[34] Seider WD, Seader JD, Lewin DR. Product & process design principles – synthesis analysis and evaluation. 3rd ed. Wiley; 2010.
[35] Turton R, Bailie RC, Whiting WB, Shaeiwitz JA. Analysis synthesis and design of chemical processes. 3rd ed. Prentice Hall; 2009.
[36] Sharma S, Rangaiah GP, Cheah KS. Multi-objective optimization using MS Excel with an application to design of a falling-film evaporator system. Food Bioprod Process 2012;90(2):123–34.
[37] Apostolakou AA, Kookos IK, Marazioti C, Angelopoulos KC. Techno-economic analysis of a biodiesel production process from vegetable oils. Fuel Process. Technol. 2009;90:1023–31.
[38] <http://www.palmoilworld.org/biodiesel.html> [accessed May 2013]..